

PROPERTIES OF DUST IN VARIOUS ENVIRONMENTS OF NEARBY GALAXIES

HIDEHIRO KANEDA¹, TAKUMA KOKUSHO¹, RIKA YAMADA¹, DAISUKE ISHIHARA¹, SHINKI OYABU¹, TORU KONDO¹, MITSUYOSHI YAMAGISHI¹, AKIKO YASUDA¹, TAKASHI ONAKA², AND TOYOAKI SUZUKI³¹Graduate School of Science, Nagoya University, Chikusa-ku, Nagoya 464-8602, Japan²Department of Astronomy, Graduate School of Science, University of Tokyo, Bunkyo-ku, Tokyo 113-0033, Japan³Netherlands Institute for Space Research, SRON, 3584 CA Utrecht, The Netherlands*E-mail: kaneda@u.phys.nagoya-u.ac.jp**(Received September 30, 2014; Revised October 20, 2016; Accepted October 20, 2016)*

ABSTRACT

We have performed systematic studies of the properties of dust in various environments of nearby galaxies with AKARI. The unique capabilities of AKARI, such as near-infrared (near-IR) spectroscopy combined with all-sky coverage in the mid- and far-IR, enable us to study processing of dust, particularly carbonaceous grains including polycyclic aromatic hydrocarbons (PAHs), for unbiased samples of nearby galaxies. In this paper, we first review our recent results on individual galaxies, highlighting the uniqueness of AKARI data for studies of nearby galaxies. Then we present results of our systematic studies on nearby starburst and early-type galaxies. From the former study based on the near-IR spectroscopy and mid-IR all-sky survey data, we find that the properties of PAHs change systematically from IR galaxies to ultra-luminous IR galaxies, depending on the IR luminosity of a galaxy or galaxy population. From the latter study based on the mid- and far-IR all-sky survey data, we find that there is a global correlation between the amounts of dust and old stars in early-type galaxies, giving an observational constraint on the origin of the dust.

Key words: Infrared: ISM — Infrared: galaxies — ISM: dust, extinction — Galaxies: ISM

1. UNIQUENESS OF AKARI DATA

For studies of nearby galaxies, AKARI has provided us with unique datasets. All-sky mid- and far-infrared (far-IR) surveys at wavelengths of 9, 18, 65, 90, 140 and 160 μm are very powerful to detect IR emission widely extended around galaxies and even into intergalactic regions. Figure 1 shows the mid- and far-IR images of the edge-on starburst galaxy, NGC 253, obtained by the all-sky surveys. They clearly exhibit IR emission widely extended to the galactic halo regions. The AKARI surveys also enable us to investigate mid- to far-IR spectral energy distributions (SEDs) for unbiased samples of nearby galaxies all over the sky.

Near-IR spectroscopy for a wavelength range of 2.5–5 μm offers valuable information on the interstellar media in galaxies with dust emission/absorption bands due to

hydrocarbon particles and ices as well as hydrogen recombination emission lines. For example, we detected galactic outflows of polycyclic aromatic hydrocarbons (PAHs) in the halos of M 82 and NGC 1569 (Yamagishi et al. 2012; Onaka et al. 2010). We found large variations in the intensity of the aliphatic emission relative to aromatic emission in the galactic superwind regions of M 82 (Yamagishi et al. 2012) and the inner galactic bar of NGC 1097 (Kondo et al. 2012), indicating systematic changes in the properties of hydrocarbon grains possibly due to large-scale shocks. We also revealed spatial variations of relative abundances of interstellar H₂O and CO₂ ices in NGC 253 and M 82, and found that they depend on the hardness of interstellar radiation field, i.e., massive star-forming activity (Yamagishi et al. 2011; Yamagishi et al. 2013).

Wide dynamic ranges of signal detection are also im-

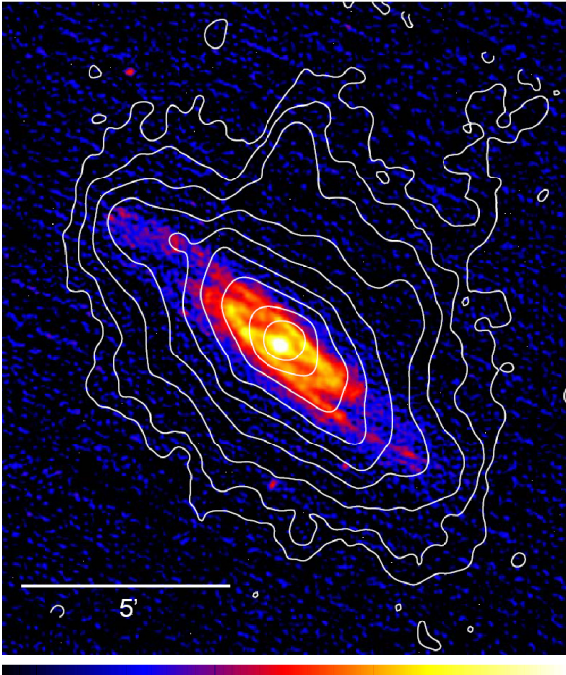


Figure 1. All-sky survey $9\ \mu\text{m}$ image of NGC 253, with the all-sky survey $90\ \mu\text{m}$ contour map. The color scale is given in a range of 0.03 % to 10 % of the $9\ \mu\text{m}$ peak intensity ($\sim 1500\ \text{MJy sr}^{-1}$), while the contour levels are from 0.03 % to 40 % of the $90\ \mu\text{m}$ peak intensity ($\sim 4100\ \text{MJy sr}^{-1}$), both drawn on a logarithmic scale.

portant characteristics of AKARI for studies of nearby galaxies; high saturation levels of the focal-plane instruments enable us to study very bright regions in galaxies, while the cryogenically-cooled 6 K telescope enables us to study low-brightness regions in galaxies. For example, we observed the starburst galaxies with prominent galactic superwinds, NGC 253 and M 82, without serious saturation problems for their very bright galactic centers. We successfully detected dust grains including PAHs widely extended in the galactic halos, which are entrained to $\sim 10\ \text{kpc}$ from the disks by galactic superwinds (Kaneda et al. 2009; Kaneda et al. 2010).

Fine allocation of many photometric bands, especially 4 bands in the far-IR, is another important merit of AKARI. The most conspicuous case is obtained by observations of Stephan’s Quintet. We found a notable difference in the spatial distribution of far-IR emission in the group of galaxies between the $160\ \mu\text{m}$ band and the other 3 bands; only in the $160\ \mu\text{m}$ band, we significantly detected emission from the intergalactic region, which is not apparently associated with any member galaxies (Suzuki et al. 2011). Following AKARI, far-IR spectroscopy by Herschel revealed a high luminosity of the [C II] $158\ \mu\text{m}$ line relative to the IR luminosity for

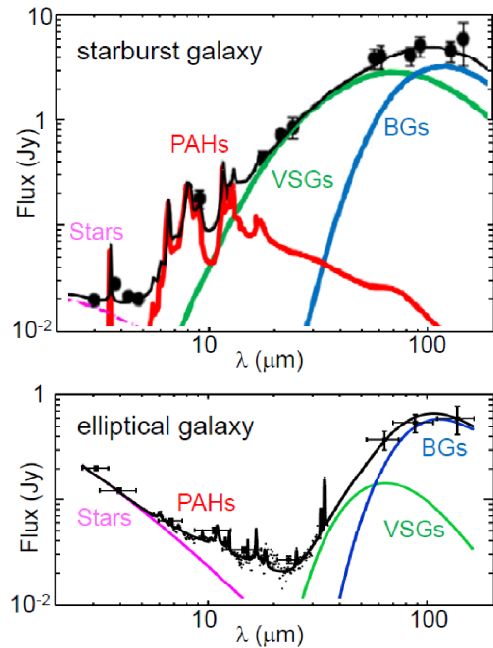


Figure 2. Typical mid- to far-IR SEDs of a starburst galaxy (MCG-02-01-051; Yamada et al. 2013) and an elliptical galaxy (NGC 4125; Kaneda et al. 2011), which are created by using not only AKARI but also Spitzer, WISE and IRAS data.

this region, which was about 30 times as bright as that in typical star-forming galaxies (Appleton et al. 2013). The unusually strong [C II] line is likely to be powered by large-scale shocks due to interaction of the galaxies in Stephan’s Quintet, which causes the above difference for the $160\ \mu\text{m}$ band. In this aspect, not only the $160\ \mu\text{m}$ band but also the $65\ \mu\text{m}$ band might be important since the latter contains the [O I] $63\ \mu\text{m}$ line; we actually detect locally-enhanced $65\ \mu\text{m}$ band intensities in the halo of M 82 (Kaneda et al. 2010).

2. SYSTEMATIC STUDIES WITH AKARI

We present examples of the results obtained by our systematic studies on nearby starburst and early-type galaxies, based on mid- and far-IR all-sky maps combined with near-IR spectra. Details of the results will be reported in separate papers. As can be seen in Figure 2, we should be careful about a large difference in the interpretation of mid-IR SEDs between star-formation active and passive galaxies; 9 and $18\ \mu\text{m}$ fluxes are dominated by PAH and very small grain (VSG) components for starburst galaxies, while they are generally dominated by a stellar component for early-type galaxies.

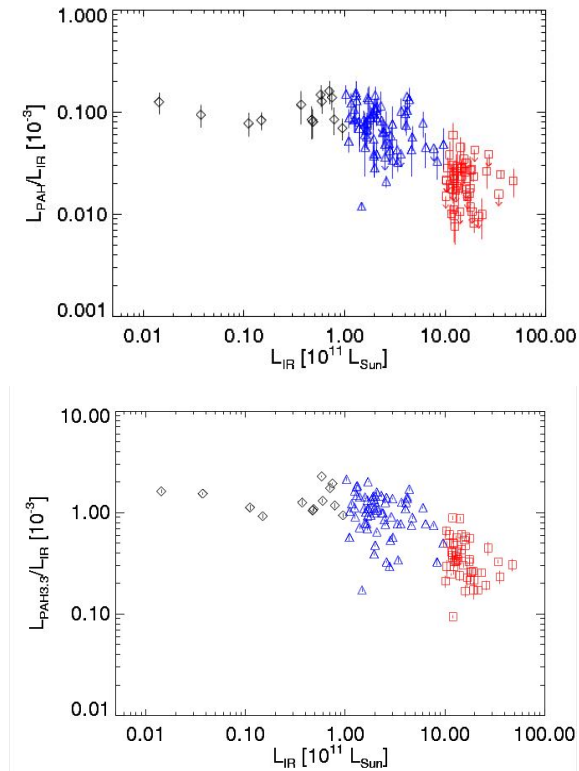


Figure 3. (Top) $L_{\text{PAH}}/L_{\text{IR}}$ and (bottom) $L_{\text{PAH}3.3}/L_{\text{PAH}}$ as a function of L_{IR} for 130 starburst galaxies. The latter plot is taken from Yamada et al. (2013). L_{PAH} and $L_{\text{PAH}3.3}$ are the total PAH band luminosity and the PAH 3.3 μm band luminosity, which are estimated by near- to far-IR SED fitting and near-IR spectral fitting, respectively.

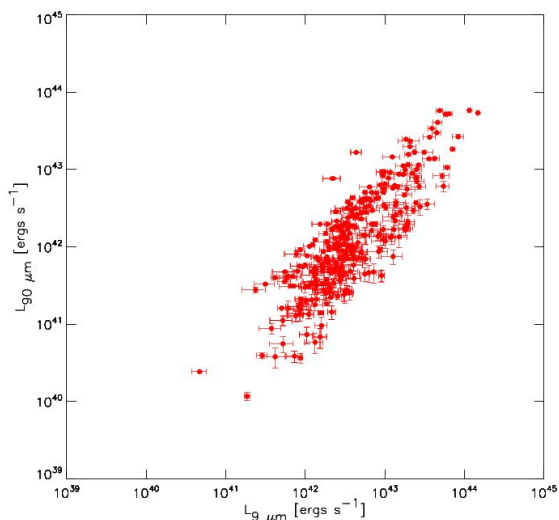


Figure 4. Scatter plot between the AKARI 90 μm and 9 μm band luminosities for 390 nearby early-type galaxies.

2.1. Processing of Dust in Starburst Galaxies

We investigate the properties of dust in star-forming galaxies with a wide range of IR luminosity. For 130 nearby starburst galaxies at redshifts < 0.17 , near- to far-IR SEDs are decomposed into PAH, VSG and big grain (BG) components by using DustEM (Compiègne et al. 2011), as shown in Figure 2. The total IR luminosity, L_{IR} , of a galaxy is estimated by adding the luminosities of the three components, L_{PAH} , L_{VSG} and L_{BG} . Then the sample is classified into IR galaxies (IRGs; $L_{\text{IR}} < 10^{11} L_{\odot}$), luminous IR galaxies (LIRGs: $L_{\text{IR}} \sim 10^{11} - 10^{12} L_{\odot}$) and ultra-luminous IR galaxies (ULIRGs: $L_{\text{IR}} > 10^{12} L_{\odot}$), where AGNs are removed based on the near-IR spectral features as described in Imanishi et al. (2010). We find that $L_{\text{PAH}}/L_{\text{IR}}$ and $L_{\text{VSG}}/L_{\text{IR}}$ systematically decrease with L_{IR} toward the luminous end in the ULIRG population; the top panel of Figure 3 shows the result for $L_{\text{PAH}}/L_{\text{IR}}$.

For each of the sample galaxies, we also estimate the PAH 3.3 μm band luminosity, $L_{\text{PAH}3.3}$, from their near-IR spectra, and then find that $L_{\text{PAH}3.3}/L_{\text{IR}}$ again decreases with L_{IR} quite similarly to $L_{\text{PAH}}/L_{\text{IR}}$, as shown in the bottom panel of Figure 3 (Yamada et al. 2013). We conclude that nearby ULIRGs intrinsically possesses smaller amounts of PAHs relative to BGs; since nearby ULIRGs are thought to be recent galaxy mergers, PAHs may have been destroyed once by shocks during a merging process, whereas BGs survive.

In addition, we find that $L_{\text{PAH}3.3}/L_{\text{PAH}}$ significantly increases with L_{IR} (IRG: 0.013 ± 0.001 , LIRG: 0.015 ± 0.001 , ULIRG: 0.019 ± 0.001), suggesting that the properties of PAHs may change with the IR luminosity or galaxy population. In general, higher $L_{\text{PAH}3.3}/L_{\text{PAH}}$ ratios can be explained by dominance of softer radiation field (i.e., neutral PAHs) or small-sized PAHs (Draine & Li 2007). However the former situation is unlikely for high IR luminosities in ULIRGs, and it is more plausible that older stellar population, which has survived the galaxy merger, starts to produce small, fresh PAHs in the ULIRGs. Hence the observed changes of L_{PAH} , $L_{\text{PAH}3.3}$ and $L_{\text{PAH}3.3}/L_{\text{PAH}}$ with L_{IR} can be explained by considering galaxy mergers and subsequent PAH evolution, especially for nearby ULIRGs.

2.2. Origins of Dust in Early-type Galaxies

In general, as compared to late-type galaxies, early-type galaxies are poor in dust, and thus relatively difficult to detect in the mid- and far-IR. Thanks to the improved sensitivities, however, AKARI detects many

early-type galaxies as well in the all-sky surveys. For 390 nearby early-type galaxies, which are reliably detected with AKARI in both 90 and 140 μm bands, we investigate the relationship between the luminosities in the different photometric bands. We confirm that the 9 μm luminosity is tightly correlated with the 18 μm luminosity, while the 90 μm luminosity is correlated with the 140 μm luminosity. These correlations are readily understood since the 9 μm and 18 μm bands trace the photospheric emission of old stars (see Figure 2), while the 90 μm and 140 μm bands trace the thermal emission of BGs. More importantly, however, we also find a tight correlation between 9 μm and 90 μm , as shown in Figure 4. This indicates that the amounts of the old stars and the cold dust are related to each other, giving an observational constraint on the origin of the dust.

In principle, the amount of dust in elliptical galaxies is determined by a balance between a dust destruction rate due to sputtering by hot plasma and a dust supply rate. If the dominant supplying source of the dust is stellar mass losses, or in other words, if gas-rich mergers are not important for the origin of the dust, the correlation between the stars and dust in Figure 4 would be reasonable. However there has been a long-standing issue that the amount of dust observed in elliptical galaxies is often too large, which is ~ 2 orders of magnitude larger than that determined by the above balance (e.g., Knapp et al. 1989; Knapp et al. 1992; Goudfrooij & de Jong 1995). We confirm such excess of dust for our sample on the basis of the AKARI data. Then, in order to explain both correlation and excess, we may require internal accumulation processes of dust in a galaxy.

Spatial information on the far-IR emission is key to understanding the origin of the dust. However the spatial resolution of AKARI is not good enough to resolve the far-IR images of the sample galaxies very well. Herschel now reveals the spatial distribution of dust in detail, but only for a handful of elliptical galaxies. The Herschel far-IR images in Figure 5 show that the dust does not follow the stellar distribution, but is concentrated near the galactic center, suggesting the importance of internal accumulation of dust near the center, possibly heated by declining nuclear activity.

3. SUMMARY

Utilizing the unique capabilities of AKARI, such as mid- and far-IR all-sky surveys and near-IR spectroscopy, we have systematically studied the properties of dust including PAHs for unbiased samples of nearby galax-

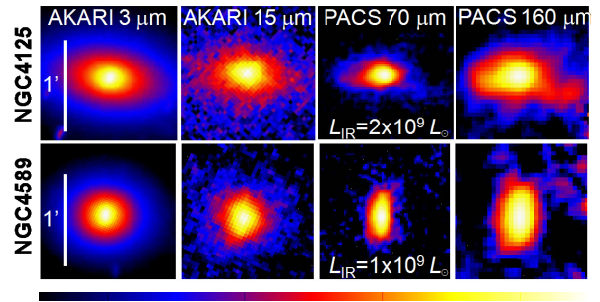


Figure 5. Near- to far-IR images of NGC 4125 and NGC 4589 obtained by AKARI and Herschel/PACS. The color scale is given in a range of 1 to 100 % of the peak brightness on a logarithmic scale.

ies. For 130 starburst galaxies, we show that not only $L_{\text{PAH}}/L_{\text{IR}}$ but also $L_{\text{PAH}3.3}/L_{\text{IR}}$ decrease with L_{IR} . Moreover we find that $L_{\text{PAH}3.3}/L_{\text{PAH}}$ increases with L_{IR} . We suggest that these changes can be explained by considering galaxy mergers and subsequent PAH evolution, especially for nearby ULIRGs. For 390 early-type galaxies, we find a global correlation between dust and stellar amounts, suggesting that stellar mass losses, but not gas-rich mergers, are important for the origin of dust. Considering short time scales of sputtering destruction of dust, we may require internal accumulation processes of dust in a galaxy; Herschel far-IR images suggest the presence of a dust reservoir near the galactic center.

ACKNOWLEDGMENTS

AKARI is a JAXA project with the participation of ESA. This research was supported by JSPS KAKENHI Grant Numbers 22340043 and 25247020.

REFERENCES

- Appleton, P. N., et al., 2013, Shock-enhanced C⁺ Emission and the Detection of H₂O from the Stephan's Quintet Group-wide Shock Using Herschel, *ApJ*, 777, 66
- Compiègne, M., et al., 2011, The global dust SED: tracing the nature and evolution of dust with DustEM, *A&A*, 525, 103
- Draine, B. T. & Li, A., 2007, Infrared Emission from Interstellar Dust. IV. the Silicate-graphite-PAH Model in the Post-Spitzer Era, *ApJ*, 657, 810
- Goudfrooij, P. & de Jong, T., 1995, Interstellar matter in Shapley-Ames elliptical galaxies. IV. A diffusely distributed component of dust and its effect on colour gradients, *A&A*, 298, 784
- Imanishi, M., Nakagawa, T., Shirahata, M., Ohyama, Y., & Onaka, T., 2010, AKARI IRC Infrared 2.5–5 μm Spec-

- troscopy of a Large Sample of Luminous Infrared Galaxies, *ApJ*, 721, 1233
- Kaneda, H., Yamagishi, M., Suzuki, T., & Onaka, T., 2009, AKARI Detection of Far-Infrared Dust Emission in the Halo of NGC253, *ApJ*, 698, L125
- Kaneda, H., et al., 2010, Large-scale distributions of mid- and far-infrared emission from the center to the halo of M82 revealed with AKARI, *A&A*, 514, A14
- Kaneda, H., Ishihara, D., Onaka, T., Suzuki, T., Mori, T., Oyabu, S., & Yamagishi, M., 2011, Properties of dust and PAHs in the hot plasma of the elliptical galaxy NGC 4125 revealed with AKARI and Spitzer Space Telescope, *PASJ*, 63, 601
- Knapp, G. R., Guhathakurta, P., Kim, D.-W., & Jura, M. A., 1989, Interstellar matter in early-type galaxies. I – IRAS flux densities, *ApJS*, 70, 329
- Knapp, G. R., Gunn, J. E. & Wynn-Williams, C. G., 1992, Infrared emission and mass loss from evolved stars in elliptical galaxies, *ApJ*, 399, 76
- Kondo, T. et al., 2012, The Central Region of the Barred Spiral Galaxy NGC 1097 Probed by AKARI Near-infrared Spectroscopy, *ApJ* L751, 18
- Onaka, T., Matsumoto, H., Sakon, I., & Kaneda, H., 2010, Detection of unidentified infrared bands in a $H\alpha$ filament in the dwarf galaxy NGC 1569 with AKARI, *A&A*, 514, A15
- Suzuki, T., Kaneda, H., Onaka, T., & Kitayama, T., 2011, Far-infrared Emission from the Intergalactic Medium in Stephan's Quintet Revealed by AKARI, *ApJ*, 731, L12
- Yamada, R., Oyabu, S., Kaneda, H., Yamagishi, M., Ishihara, D., Kim, J. -H., & Im, M., 2013, A Relation of the PAH 3.3 μm Feature with Star-forming Activity for Galaxies with a Wide Range of Infrared Luminosity, *PASJ*, 65, 103
- Yamagishi, M., Kaneda, H., Ishihara, D., Oyabu, S., Onaka, T., Shimonishi, T., & Suzuki, T., 2011, AKARI Near-infrared Spectroscopic Observations of Interstellar Ices in the Edge-on Starburst Galaxy NGC 253, *ApJ*, 731, L20
- Yamagishi, M., et al., 2012, AKARI near-infrared spectroscopy of the aromatic and aliphatic hydrocarbon emission features in the galactic superwind of M82, *A&A*, 541, 10
- Yamagishi, M., et al., 2013, Difference in the Spatial Distribution between H_2O and CO_2 Ices in M 82 Found with AKARI, *ApJ*, 773, 37